Low-frequency transmitted intensity noise induced by stimulated Brillouin scattering in optical fibers

Asaf David* **and Moshe Horowitz**

Department of Electrical Engineering, Technion–Israel Institute of Technology, Haifa 32000 Israel

*asafd@tx.technion.ac.il

Abstract: We study theoretically and experimentally the spectral properties of low-frequency transmitted intensity noise induced by stimulated Brillouin scattering in optical fibers. In fibers with a length of 25 km the Brillouin scattering induces transmitted intensity noise with a bandwidth on the order of tens of kHz. The power spectral density of the noise can be stronger than the shot noise in the photo-detector even when the optical power is significantly lower than the Brillouin threshold. The low-frequency transmitted intensity noise is caused due to depletion of the pump wave by the stochastic Brillouin wave. Since pump depletion occurs over a long distance, noise with a narrow bandwidth is generated in the transmitted wave. When the pump power is high enough, the spectrum of the induced noise contains features such as hole at low frequencies and ripples. Good quantitative agreement between theory and experiments is obtained. Low-frequency intensity noise induced by Brillouin scattering may limit the generation of ultra-low noise signals in optoelectronic oscillators and may limit the transfer of ultra-low noise signals in fibers.

OCIS codes: (290.5900) Scattering, stimulated Brillouin; (060.4370) Non-linear optics, fibers; (350.5500) Propagation; (270.2500) Fluctuations, relaxations, and noise.

References and links

1. R. Y. Chiao, C. H. Townes, and B. P. Stoicheff, "Stimulated Brillouin Scattering and Coherent Generation of Intense Hypersonic Waves," Phys. Rev. Lett. **12**, 592–595 (1964).
2. E. P. Ippen and R. H. Stolen, "Stimulated Brillouin scattering in optical fibers," Appl. Phys. Lett. **21**, 539–541 (1972).
3. R. G. Smith, "Optical power handling capacity of low loss optical fibers as determined by stimulated Raman and Brillouin scattering," Appl. Opt. **11**, 2489–2494 (1972).
4. R. W. Tkach, A. R. Chraplyvy, and R. M. Derosier, "Spontaneous Brillouin scattering for single-mode optical-fibre characterisation," Electron. Lett. **22**, 1011–1013 (1986).
5. R. W. Boyd, K. Rzążewski, and P. Narum, "Noise initiation of stimulated Brillouin scattering," Phys. Rev. A **42**, 5514–5521 (1990).
6. A. L. Gaeta and R. W. Boyd, "Stochastic dynamics of stimulated Brillouin scattering in an optical fiber," Phys. Rev. A **44**, 3205–3209 (1991).
7. A. A. Fotiadi, R. Kiyan, O. Deparis, P. Mégret, and M. Blondel, "Statistical properties of stimulated Brillouin scattering in single-mode optical fibers above threshold," Opt. Lett. **27**, 83–85 (2002).
8. L. Stépien, S. Randoux, and J. Zemmouri, "Origin of spectral hole burning in Brillouin fiber amplifiers and generators," Phys. Rev. A **65**, 053 812 (2002).
9. Y. Takushima and K. Kikuchi, "Spectral gain hole burning and modulation instability in a Brillouin fiber amplifier," Opt. Lett. **20**, 34–36 (1995).

#144143 - $15.00 USD Received 16 Mar 2011; revised 12 May 2011; accepted 12 May 2011; published 2 Jun 2011

10. M. Horowitz, A. R. Chraplyvy, R. W. Tkach, and J. L. Zyskind, "Broad-band transmitted intensity noise induced by Stokes and anti-Stokes Brillouin scattering in single-mode fibers," IEEE Photon. Technol. Lett. **9**, 124–126 (1997).
11. X. P. Mao, R. W. Tkach, A. R. Chraplyvy, R. M. Jopson, and R. M. Derosier, "Stimulated Brillouin threshold dependence on fiber type and uniformity," IEEE Photon. Technol. Lett. **4**, 66–69 (1992).
12. P. A. Williams, W. C. Swann, and N. R. Newbury, "High-stability transfer of an optical frequency over long fiber-optic links," J. Opt. Soc. Am. B **25**, 1284–1293 (2008).
13. X. S. Yao and L. Maleki, "Optoelectronic microwave oscillator," J. Opt. Soc. Am. B **13**, 1725–1735 (1996).
14. C. W. Nelson, A. Hati, D. A. Howe, and W. Zhou, "Microwave optoelectronic oscillator with optical gain," in Proc. IEEE Frequency Control Symp., pp. 1014–1019 (May 2007).
15. C. W. Nelson, A. Hati, and D. A. Howe, "Relative intensity noise suppression for RF photonic links," IEEE Photon. Technol. Lett. **20**, 1542–1544 (2008).
16. D. Eliyahu, D. Seidel, and L. Maleki, "RF amplitude and phase-noise reduction of an optical link and an opto-electronic oscillator," IEEE Trans. Microwave Theory Tech. **56**, 449–456 (2008).
17. M. O. van Deventer and A. J. Boot, "Polarization properties of stimulated Brillouin scattering in single-mode fibers," IEEE J. Lightwave Technol. **12**, 585–590 (1994).
18. E. Levy, M. Horowitz, and C. R. Menyuk, "Noise distribution in the radio-frequency spectrum of opto-electronic oscillators," Opt. Lett. **33**, 2883–2885 (2008).
19. A. Melloni, M. Frasca, A. Garavaglia, A. Tonini, and M. Martinelli, "Direct measurement of electrostriction in optical fibers," Opt. Lett. **23**, 691–693 (1998).
20. R. B. Jenkins, R. M. Sova, and R. I. Joseph, "Steady-state noise analysis of spontaneous and stimulated Brillouin scattering in optical fibers," IEEE J. Lightwave Technol. **25**, 763–770 (2007).
21. C. J. Misas, P. Petropoulos, and D. J. Richardson, "Slowing of pulses to c/10 with subwatt power levels and low latency using Brillouin amplification in a bismuth-oxide optical fiber," IEEE J. Lightwave Technol. **25**, 216–221 (2007).
22. M. Nikles, L. Thevenaz, and P. A. Robert, "Brillouin gain spectrum characterization in single-mode optical fibers," IEEE J. Lightwave Technol. **15**, 1842–1851 (1997).
23. V. Lanticq, S. Jiang, R. Gabet, Y. Jaouën, F. Taillade, G. Moreau, and G. P. Agrawal, "Self-referenced and single-ended method to measure Brillouin gain in monomode optical fibers," Opt. Lett. **34**, 1018–1020 (2009).
24. P. D. Dragic, "Simplified model for effect of Ge doping on silica fibre acoustic properties," Electron. Lett. **45**, 256–257 (2009).
25. J. H. Mathews and K. D. Fink, *Numerical Methods Using MATLAB*, 3rd ed., (Prentice Hall, 1999), Chap. 9.
26. M. G. Raymer and J. Mostowski, "Stimulated Raman scattering: unified treatment of spontaneous initiation and spatial propagation," Phys. Rev. A **24**, 1980–1993 (1981).
27. V. I. Kovalev and R. G. Harrison, "Observation of inhomogeneous spectral broadening of stimulated Brillouin scattering in an optical fiber," Phys. Rev. Lett. **85**, 1879–1882 (2000).

1. Introduction

Stimulated Brillouin scattering (SBS) has been intensively studied in bulk materials [1] and in fibers [2–4]. The scattering arises from longitudinal acoustic waves and it leads to the generation of a backward propagating Brillouin wave with a frequency that is down-shifted with respect to the frequency of the forward propagating pump wave. The intensity of the Brillouin wave fluctuates on time due to the spontaneous Brillouin scattering that initiates the process [5–8,10]. The spectrum of the Brillouin wave has been studied analytically in case that pump depletion is negligible [5]. The spectrum of the backward propagating Brillouin wave has been also studied theoretically by using numerical simulations [5, 7, 8]. In particular, effects such as spectral hole burning and ripples in the spectrum of the backward propagating Brillouin wave have been demonstrated [7–9]. These effects were also calculated for the transmitted pump wave [8]. Brillouin scattering also induces noise in the forward propagating wave in a broad frequency region of $0-1$ GHz [10, 11]. This noise is obtained due a double scattering process that is based on both stimulated and thermally excited phonons.

In this work we study theoretically and experimentally the spectral properties of low-frequency intensity noise induced in the transmitted pump wave due to SBS. The noise is induced due to the depletion of the pump wave by the noisy backward propagating Brillouin wave. Since the pump depletion occurs over a long distance, noise with a narrow bandwidth is generated in the transmitted wave. For a 25-km long optical fiber, the bandwidth of this noise

#144143 - $15.00 USD Received 16 Mar 2011; revised 12 May 2011; accepted 12 May 2011; published 2 Jun 2011

is on the order of tens of kHz and it strongly depends on the pump power. The power spectral density of noise induced by SBS can be stronger than the shot noise in the photodetector even when the optical power is significantly lower than the Brillouin threshold. When the power is high enough, the spectrum contains features such as a hole in low frequencies and ripples. Good quantitative agreement between theory and experiments is obtained. A reduced model for calculating the power spectral density of the transmitted noise is given for input powers that are close to the Brillouin threshold.

The study of low-frequency noise induced by Brillouin scattering might be important for transferring ultra-low noise signals in fibers (see for example [12]) and for generating ultra-low noise signals in optoelectronic oscillators (OEOs). To decrease phase noise in OEOs, the length of the OEO cavity and the optical power should be both increased [13]. The increase of the optical power also decreases the required RF amplifier gain and at high enough optical power the RF amplifier may even become unnecessary [14]. However, if the signal power and the fiber length are increased, Brillouin effect can induce noise in the low-frequency region that is important for applications that are based on OEOs (0−100 kHz). Hence, SBS can limit the performance of OEOs. Modulating the laser frequency [14–16] have significantly decreased the phase noise. The noise decrease was attributed to suppression of interferometric noise, stimulated Brillouin scattering, and/or further reduction of RIN [14, 15]. However, techniques for increasing the Brillouin threshold may also increase phase noise due to dispersion and other propagation effects in fibers.

2. Theoretical model

We study numerically the SBS dynamics by using the model described in Refs. [5, 6]. We present the electric field $e(z,t) = e_L(z,t) + e_S(z,t)$, where $e_L(z,t) = 1/2\{E_L(z,t)\exp(k_L z - i\omega_L t) + \text{c.c.}\}$ is the field of the forward propagating pump wave, $e_S(z,t) = 1/2\{E_S(z,t)\exp(-k_S z - i\omega_S t) + \text{c.c.}\}$ is the field of the backward propagating Brillouin wave, z is the location along the fiber, t is the time, $E_L(z,t)$ and $E_S(z,t)$ are the complex envelopes of the forward propagating pump wave and the backward propagating Brillouin wave, respectively, ω_L and k_L are the carrier frequency and the wavenumber of the pump wave, and ω_S and k_S are the carrier frequency and the wavenumber of the Brillouin wave. The propagation equations equal [5]:

$$\frac{\partial E_L(z,t)}{\partial z} + \frac{n}{c}\frac{\partial E_L(z,t)}{\partial t} = -\frac{\alpha}{2}E_L(z,t) + i\kappa E_S(z,t)\rho(z,t) \tag{1a}$$

$$\frac{\partial E_S(z,t)}{\partial z} - \frac{n}{c}\frac{\partial E_S(z,t)}{\partial t} = \frac{\alpha}{2}E_S(z,t) - i\kappa E_L(z,t)\rho^*(z,t) \tag{1b}$$

$$\frac{\partial \rho(z,t)}{\partial t} + \frac{\Gamma}{2}\rho(z,t) = i\Lambda E_L(z,t)E_S^*(z,t) + f(z,t), \tag{1c}$$

where $\rho(z,t)$ is the complex envelope of the density variation, c is the light velocity in vacuum, n is the refractive index, α is the absorption coefficient of the fiber, κ and Λ are the Brillouin coupling coefficients, Γ is the phonon decay rate, and $f(z,t)$ represents the thermal fluctuations of the medium density that initiates the spontaneous Brillouin scattering. We assume that $f(z,t)$ is a white Gaussian noise with zero mean and with no correlation in both time and space such that $< f(z,t)f^*(z',t') >= Q\delta(z-z')\delta(t-t')$, where δ is Dirac delta function, $Q = (2k_B T\rho_0\Gamma)/(V_A^2 A_{eff})$ characterizes the strength of the thermal fluctuations, k_B is Boltzmann constant, T is the temperature, V_A is the velocity of sound in the fiber, ρ_0 is the average density, and A_{eff} is the effective area of the fiber. Polarization effect reduces the effective Brillouin coefficient [17]. We take this effect into account when we determine the fiber parameters.

#144143 - $15.00 USD Received 16 Mar 2011; revised 12 May 2011; accepted 12 May 2011; published 2 Jun 2011

We note that in this manuscript we use the MKS system of units. Therefore, the relation between the intensity and the field is given by $I(z,t)=\varepsilon_0 cn|E(z,t)|^2/2$, where ε_0 is the vacuum permittivity. To calculate the transmitted RF power spectrum we assume that the output voltage equals $v(t)=\eta I(z=L,t)A_{\rm eff}R$ where R=50 Ω is the load impedance, L is the fiber length, η is the responsivity of the photodetector, and $A_{\rm eff}$ is the effective area of the fiber. The power spectral density of the noise is calculated by:

$$S_{RF}=\frac{2}{R\tau}\left|\int_0^{\tau} v(t)\exp\left(-2\pi i f t\right)dt\right|^2, \tag{2}$$

where τ is the duration of the simulated signal and f is the RF frequency. The spectrum in Eq. (2) was multiplied by a factor of two since we calculate the one-sided spectrum. We note that since τ is finite we actually calculate the periodogram and not the power spectral density. The periodogram is only an estimation of the power spectral density and it contains additional small fluctuations. Similar fluctuations are also obtained in experiments due to the finite duration of the measurement [18].

In our experiments we measured the noise induced by Brillouin scattering in a standard single-mode fiber (Corning SMF-28) at a wavelength $\lambda=1.55$ μm. Therefore, we used in our simulations the parameters for that fiber that were measured in previous works. We assume $A_{\rm eff}=80\mu{\rm m}^2$ and $n=1.45$. The measured attenuation in our fiber equals $\alpha=0.25$ dB/km. The Brillouin parameter Λ was calculated by using the equation $\Lambda=\gamma q^2\varepsilon_0/4\Omega$, where q is the acoustic wave number, $q\simeq 2\omega n/c$, Ω is the acoustic frequency, and $\gamma=0.902$ is the elctrostrictive constant [19]. The measured Brillouin frequency offset that was measured in our experiments equals $\Omega=10.86$ GHz. The constant κ was calculated from the Brillouin gain coefficient g_B [5, 20] that can be directly measured in experiments:

$$g_B=\frac{8\kappa\Lambda}{\varepsilon_0 cn\Gamma}=\frac{\gamma^2\omega^2}{nV_A c^3\rho_0\Gamma}. \tag{3}$$

In case of complete polarization scrambling in low-birefringent fibers the Brillouin gain is reduced by a factor of M=3/2 in compared with the case that polarization is preserved [17]. In previous works, the gain coefficient varies between $g_B=1.3\cdot 10^{-11}$m/W [21] to $g_B=2.6\cdot 10^{-11}$m/W [22]. A gain coefficient $g_B=1.68\cdot 10^{-11}$ m/W was measured in Ref. [23]. In our simulations we assumed $g_B=(1.68\cdot 10^{-11}/M)$ m/W. We also assumed $\rho_0=2210$ kg/m^3 and $V_a=5800$ m/s [24] to calculate the thermal fluctuation amplitude Q. The phonon decay rate was set to $\Gamma/(2\pi)=30$ MHz as in [24]. In all of our calculations we set the photodetector responsivity to $\eta=1$ A/W and the load impedance to $R=50\Omega$.

We have solved equations (1) numerically by using the Finite Difference Time Domain (FDTD) method [25] with a spatial step size $\Delta z=1$ m and a temporal step size $\Delta t=\Delta z n/c$. In each step, the pump and the backward Brillouin wave were propagated in opposite directions. We used the following boundary conditions: $E_L(z=0,t)=\sqrt{2P_0/(\varepsilon_0 cnA_{\rm eff})}$, $E_S(z=L,t)=0$, where P_0 is the input optical power of the pump wave. At the beginning of the simulation we assumed that $E_S(z,t<0)=0$. The spectrum calculation was performed on the calculated data that was obtained after a duration that corresponds to 10 roundtrips in the fiber in order to ensure that initial conditions do not significantly affect the results. High accuracy of the simulation requires a sufficient small step size. We checked that by taking smaller step sizes than $\Delta z=1$ m, we did not obtain a significant change in the calculated spectrum. The results of the simulation were also in good agreement with the steady state solution for the spatial dependence of the pump and the Brillouin wave intensities [20]. To calculate the power spectrum at low frequencies we had to simulate the propagation for a long duration of 34 ms. Therefore,

#144143 - $15.00 USD Received 16 Mar 2011; revised 12 May 2011; accepted 12 May 2011; published 2 Jun 2011

7,000,000 iterations were used in each simulation and the frequency resolution approximately equals $\Delta f = 30$ Hz.

Figure 1 shows the average optical power of the transmitted pump and the backward propagating Brillouin wave at $z = 0$ as a function of the input power for a fiber with a 25 km length and for a fiber with a 6 km length. The results were calculated by solving numerically Eq. (1) and performing a time average of the optical powers for a period of 34 ms. To verify the results we measured the power of the transmitted pump and the backward propagating Brillouin wave for the 25-km long fiber by using our experimental setup that is described in the next session. The experimental results (green-dashed line) are in a very good agreement with the simulation results (blue-solid line). We define the SBS threshold as the input optical pump power P_{th} that gives a Brillouin wave with a power of 1% P_{th} at the input of the fiber $(z = 0)$. The threshold for the 25-km and the 6-km fibers was 4.2 mW (6.2 dBm) and 11.5 mW (10.6 dBm), respectively. The results shown in Fig. 1 are also in a very good quantitative agreement with the steady state solution given in Ref. [20].

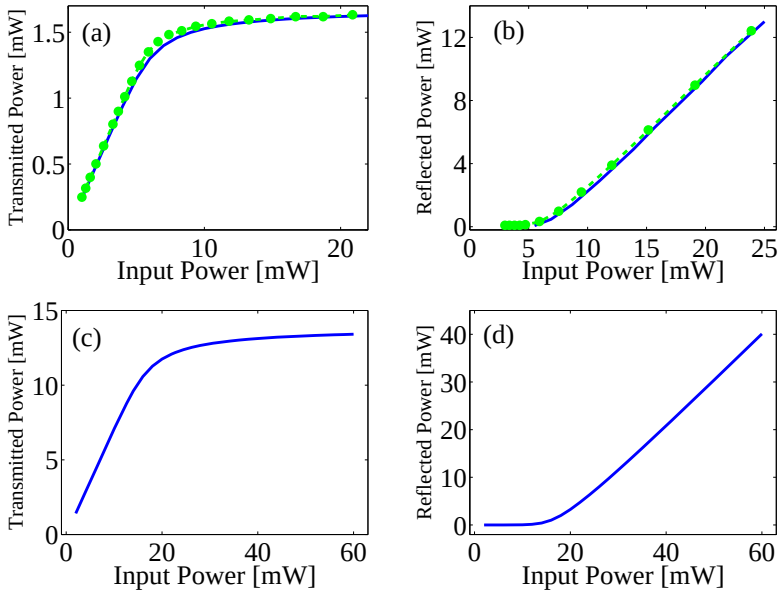

Fig. 1. Calculated average optical power of the transmitted pump wave and the backward propagating Brillouin wave at $z = 0$ as a function of the incident optical pump power for (a,b) a 25-km long fiber and for (c,d) a 6-km long fiber. The results for the 25-km fiber are compared to experimental results (green-dashed line).

Figure 2 shows the calculated RF power spectrum of the transmitted pump wave and the backward propagating Brillouin wave for three input optical powers above threshold for a fiber with a length of 25 km. The transmitted RF power spectrum is also compared to a Lorentzian function $F(f) = F_0/[1 + (f/f_0)]^2$, where the parameters F_0 and f_0 were extracted to obtain the best fit to the calculated spectra. The comparison shows that above a certain frequency, on the order of few tens of kHz, the power spectrum can be approximated by a Lorentzian function. The bandwidth f_0 of the fitted Lorentzian equals f_0=10, 20.5, and 29 kHz for input optical powers of 6.6, 16.6, and 26.3 mW, respectively. Therefore, the bandwidth of the power spectrum becomes wider as the input power increases. The power spectrum of the transmitted wave is also significantly narrower than that of the back-reflected Brillouin wave. Figure 3

#144143 - $15.00 USD Received 16 Mar 2011; revised 12 May 2011; accepted 12 May 2011; published 2 Jun 2011

shows the transmitted RF spectra for different input optical powers for a fiber with a length of 6 km and for a fiber with a length of 25 km. We note that higher frequency noise components in the frequency region on the order of hundreds of MHz are also obtained due to double scattering process that is based on both stimulated and thermally excited phonons [10].

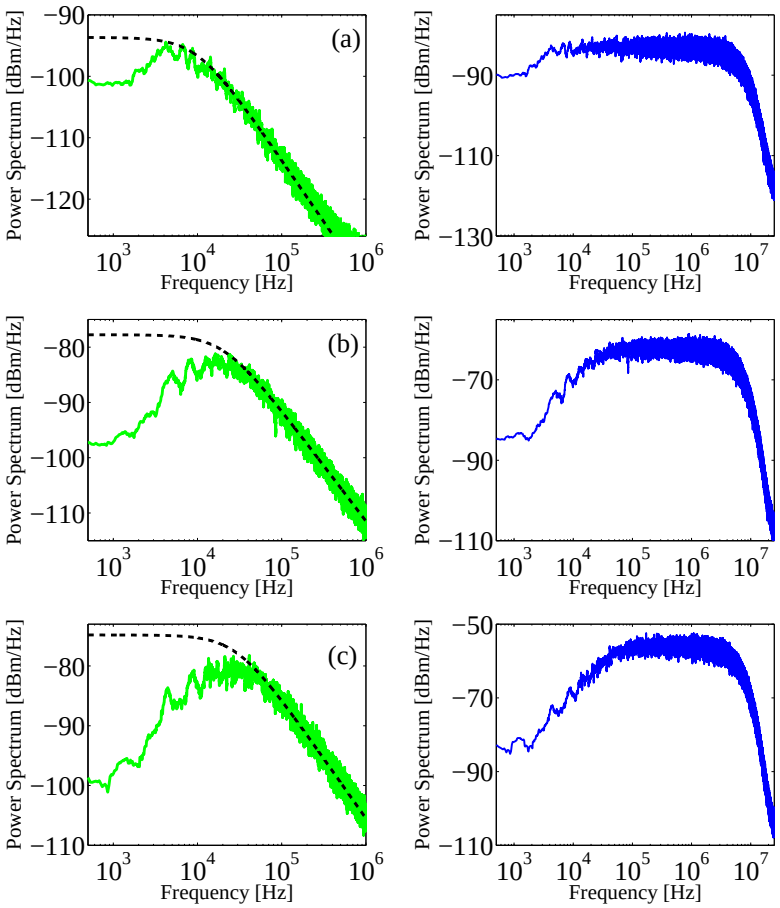

Fig. 2. RF power spectrum of the transmitted wave (left column) and of the back-reflected Brillouin wave (right column) calculated for a 25-km fiber for different input optical powers: (a) $P_0 = 6.6$ mW , (b) $P_0 = 16.6$ mW, and (c) $P_0 = 26.3$ mW. A fit of a Lorentzian function to the transmitted wave power spectrum is added (black dashed-lines). The Lorentzian bandwidths equal (a) 10 kHz, (b) 20.5 kHz, and (c) 29 kHz.

Figure 4 shows the bandwidth of the fitted Lorentzian function as a function of the fiber length. The input power for each fiber length was chosen to obtain the same small signal gain $G = g_B P_0 L_{\text{eff}}/A_{\text{eff}} = 31.2$, where $L_{\text{eff}} = [1-\exp(-\alpha L)]/\alpha$ is the effective fiber length. The ratio between the time-averaged Brillouin power at z=0 and the input power was equal 0.45 ± 0.01 for all the fiber lengths. The figure shows that the bandwidth of the transmitted spectrum is inversely proportional to the fiber length. When the fiber length is about 18 km, the Lorentzian bandwidth decreases to 42 kHz compared to 90 kHz for a fiber with a length of 6 km. The decrease is obtained since in long fibers the pump depletion occurs over longer distances.

Figures 2 and 3 show that a hole in the low-frequency region of the transmitted wave spectrum is obtained. Similar hole has been also observed in the backward Brillouin wave [7,8,27],

#144143 - $15.00 USD Received 16 Mar 2011; revised 12 May 2011; accepted 12 May 2011; published 2 Jun 2011

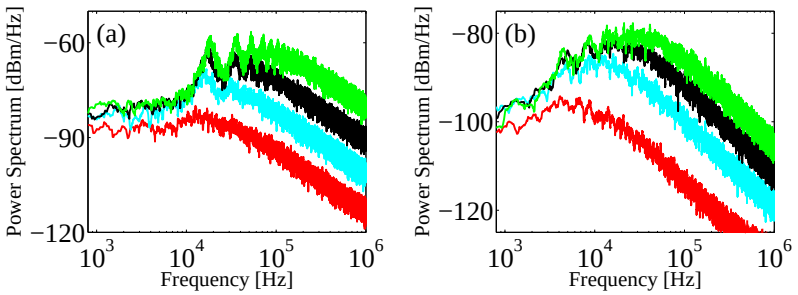

Fig. 3. RF power spectrum of the transmitted wave calculated for (a) a fiber with a length of 6 km and input optical powers of 15 mW (red), 20 mW (light blue), 30 mW (black), and 60 mW (green) and (b) calculated for a fiber with a length of 25 km and input optical powers of 6.6 mW (red), 10.5 mW (light blue), 16.6 mW (black), and 26.3 mW (green).

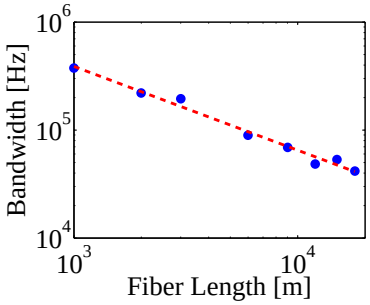

Fig. 4. Bandwidth of the fitted Lorentzian function (blue dots) as a function of the fiber length. The same small signal Brillouin gain was used for all the fiber lengths: $G = g_B P_0 L_{\text{eff}}/A_{\text{eff}} = 31.2$ and the ratio between the time-averaged Brillouin power and the input power was equal 0.45 ± 0.01. A linear fit (dashed-red line) shows that the bandwidth is inversely proportional to the fiber length.

and in the transmitted pump wave [8]. However, for long fibers ($L \gtrsim 1$ km), the hole in the transmitted wave power spectrum is narrower than that obtained in the spectrum of the Brillouin wave as shown in Fig. 2. We note that the hole can be observed at an input power that is close to the Brillouin threshold. For example, for the 6-km fiber, a 5-dB hole can be clearly observed in Fig. 3 for an input power of 15 mW. At this input power the ratio between the reflected Brillouin power and the input power equals only 6 %. The spectral hole in both the reflected and the transmitted waves was obtained by solving Eqs. (1). These equations do not contain inhomogeneous spectral broadening, as suggested in [27]. Another feature that is obtained both in the transmitted pump and in the Brillouin wave spectra is ripples that can be observed in Fig. 3. The frequency difference between the ripples in the transmitted wave equals about 17.5 kHz for the 6-km fiber and 4.3 kHz for the 25-km fiber. The frequency difference approximately equals to the round trip time, $c/2nL$, of 17.1 kHz for the 6-km fiber and 4.1 kHz for the 25-km fiber as was also previously obtained for the backward Brillouin wave [8,9]. Figure 3 also shows that the amplitude of the ripples for the 6-km fiber is higher than obtained for the 25-km fiber. This effect is caused since the total fiber loss increases as the fiber length is increased.

Figures 5(a)–5(d) show the RF power spectrum of the transmitted pump wave as a function of the input optical power calculated at several discrete frequencies of 1 kHz, 10 kHz, 17.5

#144143 - $15.00 USD Received 16 Mar 2011; revised 12 May 2011; accepted 12 May 2011; published 2 Jun 2011

kHz and 100 kHz. The noise is compared to the one-sided spectral density of the shot noise that is generated in the photodetector: $S_{SN} = 2i_{av}q_eR$, where i_{av} is the average photodetector current, $R = 50\Omega$ is the load resistance, and q_e is the electron charge. The figure shows that the noise induced by Brillouin effect is stronger than the shot noise even when the input optical power is significantly lower than the 1% optical threshold power for the 6-km fiber, $P_{th} = 11.5$ mW. However, at such low input power, noise sources that are not included in Eq. (1) such as Rayleigh scattering or noise generated by the laser can be the dominant sources of noise in the system. Due to the spectral hole in the noise spectrum the noise induced by SBS in lower frequencies might be smaller than the noise in higher frequencies. For example, the noise power spectral density at 1 kHz equals -83 dBm/HZ while the noise power spectral density at 10 kHz equals -77 dBm/Hz for an optical pump power of 20 mW. At 17.5 kHz, the ripple in the spectrum significantly increases the noise at sufficient power ($\gtrsim 17$ mW).

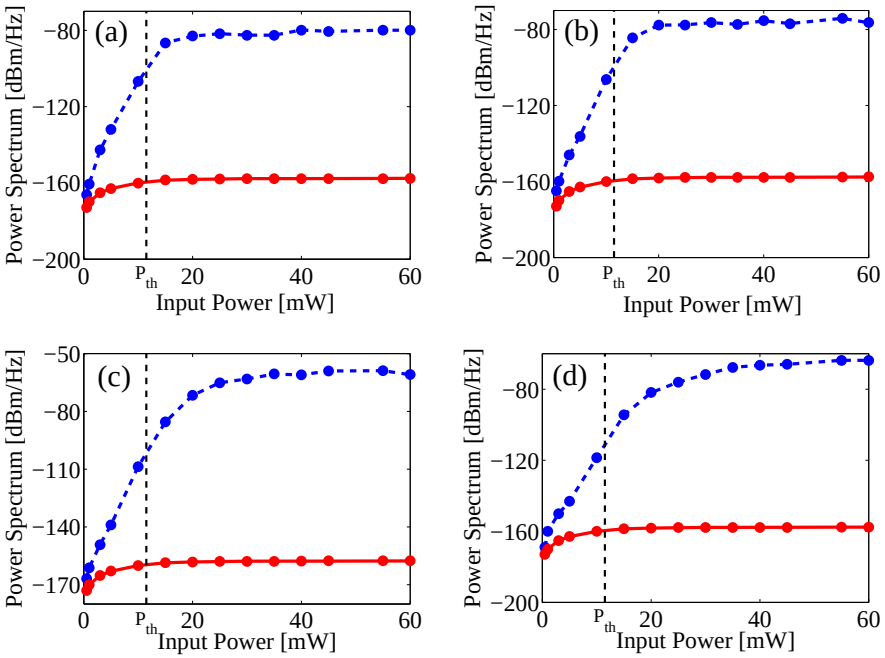

Fig. 5. RF Power spectrum (blue-dashed-line) of the transmitted wave as a function of the input optical power calculated for a 6-km fiber at frequencies (a) 1 kHz , (b) 10 kHz, (c) 17.5 kHz, and (d) 100 kHz. The calculated power spectral density is compared to the shot noise power spectral density (red-solid-line) at the output of the photodetector.

Figure 6(a) shows the bandwidth of the Lorentzian function that is fitted to the RF spectrum as a function of the input power for the 6-km fiber. The Lorentzian function was fitted even when the spectrum contained a hole and ripples as shown in Fig. 2. The figure shows that the bandwidth approximately linearly depends on the input power for a broad input power region of 7–60 mW. This result is obtained due to the pump depletion caused by the noisy Brillouin wave. The backward propagating Brillouin wave has a stochastic dynamics since it is initiated by thermal fluctuations in the density of the medium [5]. The results of the numerical simulation indicate that when the input power is in the region of 7–60 mW (the 1% threshold equals 11.5 mW) the intensity of the Brillouin wave near the fiber entrance can be approximated by an exponential function $I(z) = I(z = 0)\exp(-z/L_B)$ where L_B is defined as the buildup length

#144143 - $15.00 USD Received 16 Mar 2011; revised 12 May 2011; accepted 12 May 2011; published 2 Jun 2011

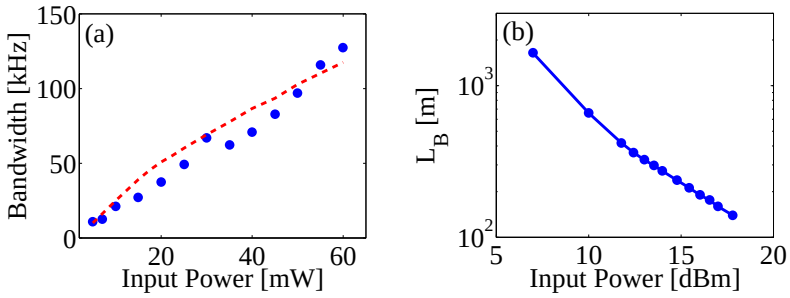

Fig. 6. (a) Bandwidth of the Lorentzian function that is fitted to the RF power spectrum of the transmitted pump wave (blue line) as a function of the input optical power. The Lorentzian bandwidth is also compared to the relation $c/4\pi nL_B$ (dashed-red line). (b) Buildup length of the backward propagating Brillouin wave, L_B, as a function of the input optical power P_0. The fiber length equals 6 km.

of the Brillouin wave. Figure 6(b) shows the buildup length of the Brillouin wave that was extracted from the numerical simulation as a function of the input optical power. At lower powers ($P < 12$ dBm) the buildup length approximately equals to the result obtained under the undepleted pump approximation, $A_{\text{eff}}/g_B P_0$ [5, 26]. The extracted depletion length of the pump wave was significantly longer than the buildup length of the Brillouin wave for optical powers that are less than 17.8 dBm (60mW). The bandwidth of the Brillouin wave is also significantly broader than the bandwidth of the transmitted intensity noise as can be seen in Fig. 2. Therefore, the noise power spectrum of the transmitted wave can be approximated as an integral of a broadband white noise that decays exponentially with a time constant of $2L_B n/c$. Note that a factor of two was added since the pump and the Brillouin wave propagate at opposite directions. Hence, at frequencies where the hole and the ripples do not affect the spectrum, the transmitted noise spectrum is approximately Lorentzian with a bandwidth of $BW = c/4\pi nL_B$. Figure 6(a) compares the relation $BW = c/4\pi nL_B$ to the bandwidth of the Lorentzian function that was extracted from the results of the numerical simulations. The figure shows that the relation is valid for input power of about 7–60 mW. At higher input optical powers the pump depletion becomes significant and the assumptions that yield the approximate mathematical relation become inaccurate.

The results of the numerical simulation can be understood by a reduced model. In case that (a) Brillouin gain is high $g_B I_L L_{\text{eff}} \gg 1$, (b) pump depletion can be neglected, (c) the power of the transmitted noise is very small in compare with the average pump power, (d) the bandwidth of the Brillouin wave is significantly broader than the bandwidth of the transmitted noise, (e) the hole and the ripples in the spectrum can be neglected, and (f) the loss in the fiber is small such that $\alpha \ll L_B^{-1}$, an explicit expression for the RF spectrum can be obtained. By using assumptions (a) and (b) the spatial dependence of the Brillouin wave near the fiber entrance can be approximated by an exponential function [5]. This result is accurate for input powers that are close to Brillouin threshold. By using assumptions (d) and (e) the Brillouin wave can be modeled as white noise. The RF power spectral density can be calculated by using the results for the Brillouin wave in [26] and calculating the Fourier transform of the autocorrelation function for the transmitted noise:

$$S_{\text{RF}}(f) \propto \frac{R\eta^2 P_S^2}{1+(4\pi n f A_{eff}/P_0 g_B c)^2}\ , \tag{4}$$

where P_S is the Brillouin wave power at the fiber entrance ($z = 0$). We note that since the pump

#144143 - $15.00 USD Received 16 Mar 2011; revised 12 May 2011; accepted 12 May 2011; published 2 Jun 2011

and Brillouin wave propagate at opposite directions, noise with a frequency f in the Brillouin wave causes a depletion at a frequency $f/2$ in the pump wave. A detailed description of the model will be given elsewhere. A comparison between the reduced model and the results of the numerical simulation shows that for the 6-km fiber at power above 15 mW the RF spectrum is strongly affected by the hole and the reduced model becomes inaccurate at low frequencies. For example, at an input power of 15 mW the ratio between P_s/P_0 = 6 % and the hole reduces the spectrum power density by about 5-dB. At low input power, below 9 mW, the assumption of an exponential buildup of the Brillouin wave becomes inaccurate. Therefore, the reduced model is accurate at the power region of 9 to 15 mW. At higher frequencies ($f \gtrsim 50$ kHz) that are not around the ripples in the spectrum, a very good agreement between the reduced model and the numerical results is obtained over a broader power region of $9-25$ mW. In this frequency region the hole does not affect the spectrum.

3. Experimental results

In our experiments we used the experimental setup shown in Fig. 7 in order to measure the power spectrum of the transmitted pump wave. A continuous wave distributed feedback laser that had a linewidth of 1 MHz, a maximum power of 40 mW, and a wavelength of 1.55 μm, was injected into a 25-km of standard fiber (Corning SMF-28). The laser power was controlled by using an optical attenuator and not by changing the laser current in order not to change the laser characteristics as a function of the power. The transmitted wave was measured by an RF spectrum analyzer that was connected to a photodetector. When the spectrum of the transmitted wave was measured, optical isolators were fused to both ends of the fiber to prevent back-reflections. Such back-reflections may increase the amplitude of the ripples in the spectrum [8]. When the back-reflected optical power was measured the isolator at the fiber input was not connected.

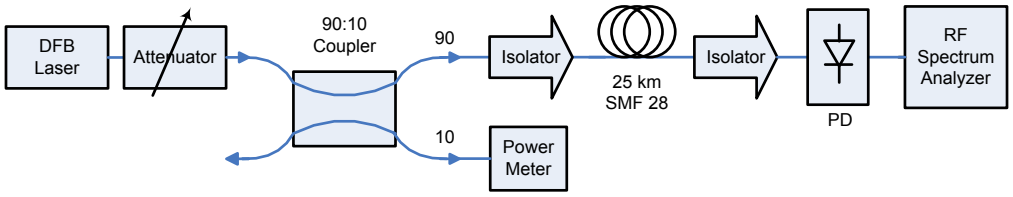

Fig. 7. Experimental setup used for measuring the RF power spectrum of the transmitted pump wave.

The experimental and the theoretical spectra are compared in Figs. 8 and 9 for several input powers. The figures show that a good quantitative agreement is obtained between theory and experiments. Features such as hole in the low frequency region of the power spectrum and ripples are obtained both in experiments and in the theoretical results.

#144143 - $15.00 USD Received 16 Mar 2011; revised 12 May 2011; accepted 12 May 2011; published 2 Jun 2011

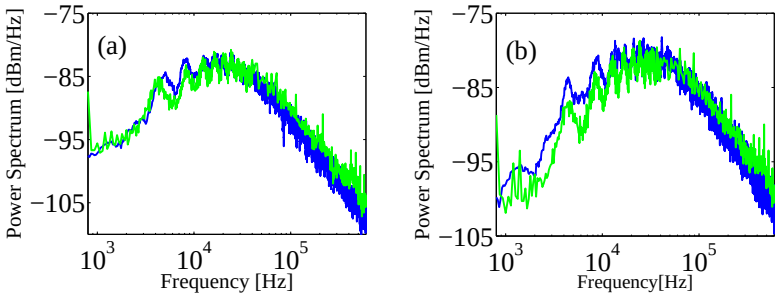

Fig. 8. Comparison between theoretical (blue line) and measured (green line) RF power spectra of the transmitted pump wave in the frequency region of 1 kHz−1 MHz for two input optical powers: (a) $P_0 = 16.6$ mW, and (b) $P_0 = 26.3$ mW. The fiber length equals 25 km. The hole in the theoretical spectrum is in a good quantitative agreement with experimental results.

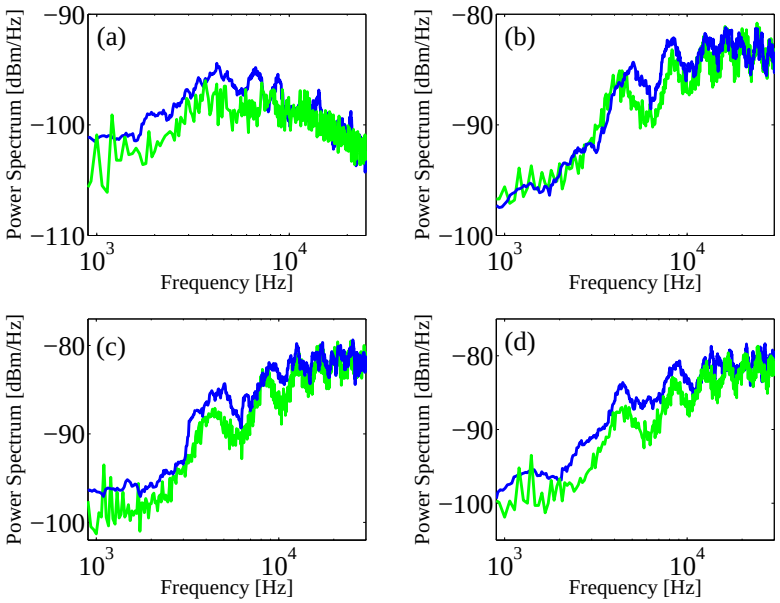

Fig. 9. Comparison between theoretical (blue line) and measured (green line) RF spectra of the transmitted pump wave in the frequency region of 800 Hz−30 kHz for four input optical powers: (a) $P_0 = 10.5$ mW, (b) $P_0 = 16.6$ mW, (c) $P_0 = 20.8$ mW, and (d) $P_0 = 26.3$ mW. The fiber length equals 25 km. The ripples in the theoretical power spectrum are in a good agreement with experimental results.

4. Conclusions

We have studied numerically and experimentally the spectral properties of low-frequency intensity noise induced by stimulated Brillouin scattering in the forward propagating transmitted pump wave. The noise is caused due to depletion of the pump wave by the stochastic Brillouin wave. The bandwidth of the noise is on the order of tens of kHz for a fiber with a length of 25 km. The bandwidth of the noise linearly increases as the pump power increases. Features such

#144143 - $15.00 USD Received 16 Mar 2011; revised 12 May 2011; accepted 12 May 2011; published 2 Jun 2011

as spectral hole at the low frequency region and ripples with a frequency difference that depends on the fiber length were theoretically and experimentally observed. Our experimental results are in a good quantitative agreement with theory. A reduced model for calculating the noise power spectral density when the input power is close to Brillouin threshold is given. The noise induced by Brillouin effect can be significantly larger than the shot noise even when the optical pump power is significantly lower than the Brillouin threshold. Noise induced by Brillouin scattering may limit the transfer of signals with ultra-low phase noise in long fibers. The frequency of the low-frequency transmitted noise induced by SBS is in the frequency region of interest for applications that are based on optoelectronic oscillators (0-100 kHz). Therefore, noise induced by Brillouin scattering may limit the performance of optoelectronic oscillators. Modulation of the laser frequency can increase the Brillouin threshold. However, such technique may also increase the phase noise in optoelectronic oscillators due to dispersion and other propagation effects in fibers. Beside Brillouin scattering there are other low-frequency noise sources such as Rayleigh scattering and noise generated by the laser that can affect the performance of OEOs. These noise sources should be included in the model to accurately model OEOs in case that the optical power is lower than the Brillouin threshold.

Acknowledgments

This work was supported by the Israel Science Foundation (ISF) of the Israeli Academy of Sciences.

#144143 - $15.00 USD Received 16 Mar 2011; revised 12 May 2011; accepted 12 May 2011; published 2 Jun 2011